Genomic and physiological footprint of the *Deepwater Horizon* oil spill on resident marsh fishes

Andrew Whitehead[a,1], Benjamin Dubansky[a], Charlotte Bodinier[a], Tzintzuni I. Garcia[b], Scott Miles[c], Chet Pilley[d], Vandana Raghunathan[e], Jennifer L. Roach[a], Nan Walker[e], Ronald B. Walter[b], Charles D. Rice[f], and Fernando Galvez[a]

Departments of [a]Biological Sciences, [c]Environmental Sciences, and [e]Oceanography and Coastal Sciences, and [d]Coastal Studies Institute, Louisiana State University, Baton Rouge, LA 70803; [b]Department of Chemistry and Biochemistry, Texas State University, San Marcos, TX 78666; and [f]Department of Biological Sciences, Clemson University, Clemson, SC 29634

Edited by Paul G. Falkowski, Rutgers, The State University of New Jersey, New Brunswick, NJ, and approved September 1, 2011 (received for review June 13, 2011)

The biological consequences of the *Deepwater Horizon* oil spill are unknown, especially for resident organisms. Here, we report results from a field study tracking the effects of contaminating oil across space and time in resident killifish during the first 4 mo of the spill event. Remote sensing and analytical chemistry identified exposures, which were linked to effects in fish characterized by genome expression and associated gill immunohistochemistry, despite very low concentrations of hydrocarbons remaining in water and tissues. Divergence in genome expression coincides with contaminating oil and is consistent with genome responses that are predictive of exposure to hydrocarbon-like chemicals and indicative of physiological and reproductive impairment. Oil-contaminated waters are also associated with aberrant protein expression in gill tissues of larval and adult fish. These data suggest that heavily weathered crude oil from the spill imparts significant biological impacts in sensitive Louisiana marshes, some of which remain for over 2 mo following initial exposures.

ecological genomics | ecotoxicology | microarray | RNA-seq | toxicogenomics

Following the *Deepwater Horizon* (DWH) drilling disaster on April 20, 2011, in the Gulf of Mexico, acute oiling and the resulting mortality of marine wildlife were evident. In contrast, the sublethal effects, critically important for predicting long-term population-level impacts of oil pollution (1), have not been well described following the DWH disaster. Here, we report the results of a 4-mo field study monitoring the biological effects of oil exposure on fish resident in Gulf of Mexico coastal marsh habitats.

Gulf killifish (*Fundulus grandis*) were used as our model species because they are among the most abundant vertebrate animals in Gulf of Mexico-exposed marshes (2–4). Furthermore, the Atlantic-distributed sister species to *F. grandis* (*Fundulus heteroclitus*) has a narrow home range and high site fidelity, especially during the summer (5, 6), and, among fishes, it is relatively sensitive to the toxic effects of organic pollutants (7). Although home range and toxicology studies are lacking for *F. grandis*, we infer that *F. grandis* is also relatively sensitive to pollutants and exhibits high site fidelity, such that the biology of this species is likely affected primarily by the local environment, given the recent shared ancestry of *F. grandis* with *F. heteroclitus* (8) and similar physiology, life history, and habitat (9–13). We sampled from populations resident in Gulf of Mexico-exposed marshes before oil landfall (May 1–9, 2010), during the peak of oil landfall (June 28–30, 2010), and after much of the surface oil was no longer apparent 2 mo later (August 30–September 1, 2010) at six field sites from Barataria Bay, Louisiana, east to Mobile Bay, Alabama (Fig. 1 and Dataset S1).

Results and Discussion

Remote sensing and analytical chemistry were used to characterize exposure to DWH oil, where remote sensing data are spatially and temporally comprehensive but of low resolution and chemistry data are of high resolution but patchy in space and time. Ocean surface oil was remotely detected through the analysis of images from synthetic aperture radar (SAR) (14). Proximity of the nearest oil slick to each field site (e.g., Fig. S1) was measured for each day that SAR data were available, from May 11 through August 13, 2010, to approximate the location, timing, and duration of coastal oiling (Fig. 1*C*). Although surface oil came close to many of our field sites in mid-June, only the Grande Terre (GT) site was directly oiled (Fig. 1 *B* and *C*). Although the GT site had been clearly contaminated with crude oil for several weeks before our sampling (Fig. 1*C* and Fig. S2) and retained much oil in sediments (Dataset S2), only trace concentrations of oil components were detected in subsurface water samples collected from the GT site on June 28, 2010, and tissues did not carry abnormally high burdens of oil constituents at any site or time point (Dataset S2). Despite a low chemical signal for oil in the water column and tissues at the time of sampling, we detected significant biological effects associated with the GT site postoil.

We sampled multiple tissues from adult Gulf killifish (average weight of 3.5 g) from each of six field sites for each of three time points [only the first two time points for the Mobile Bay (MB) site] spanning the first 4 mo of the spill event (Fig. 1*C*). We compared biological responses across time (before, at the peak, and after oiling) and across space (oiled sites and sites not oiled) and integrated responses at the molecular level using genome expression profiling with complimentary protein expression and tissue morphology. Genome expression profiles, using microarrays and RNAseq, were characterized for livers because the organ is internal and integrates xenobiotic effects from multiple routes of entry (gill, intestine, and skin), and because liver is the primary tissue for metabolism of toxic oil constituents. Tissue morphology and expression of CYP1A protein, a common biomarker for exposure to select polycyclic aromatic hydrocarbons (PAHs), was characterized for gills, the organ that provides the greatest surface area in direct contact with the surrounding aquatic environment. In addition, we exposed developing embryos to field-collected water samples to document bioavailability and bioactivity of oil contaminants for this sensitive early life stage.

Author contributions: A.W. and F.G. designed research; A.W., B.D., C.B., T.I.G., S.M., C.P., V.R., J.L.R., N.W., R.B.W. and F.G. performed research; C.D.R. contributed new reagents/analytic tools; A.W., B.D., C.B., T.I.G., S.M., C.P., V.R., N.W., R.B.W. and F.G. analyzed data; and A.W., B.D., C.B., and F.G. wrote the paper.

The authors declare no conflict of interest.

This article is a PNAS Direct Submission.

Data deposition: Microarray data have been deposited to ArrayExpress (accession no. E-MTAB-663).

[1]To whom correspondence should be addressed. E-mail: andreww@lsu.edu.

This article contains supporting information online at www.pnas.org/lookup/suppl/doi:10.1073/pnas.1109545108/-/DCSupplemental.

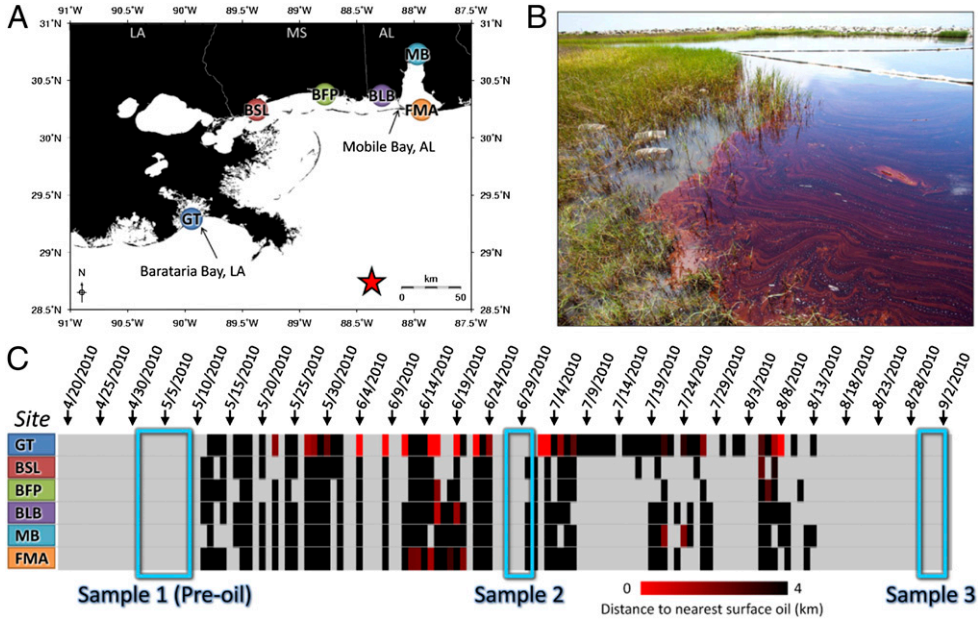

Fig. 1. Location of field study sites and incidence of oil contamination. (*A*) Location of field sampling sites, which include Grand Terre (GT), Bay St. Louis (BSL), Belle Fontaine Point (BFP), Bayou La Batre (BLB), Mobile Bay (MB), and Fort Morgan (FMA). Color coding is consistent with other figures. The red star indicates the DWH spill site. (*B*) Photograph (by A.W.) of the GT field site on June 28, 2010, showing contaminating oil and minnow traps in the marsh. (*C*) Proximity of nearest surface oil to each field site was determined by SAR, where rows are field sites and columns are days. Light gray represents no data, and black represents the nearest surface oil at a distance of >4 km; the increasing intensity of red indicates closer proximity of oil. Three field sampling trips are highlighted (blue boxes). BSL; BFP; FMA.

The oiling of the GT site at the end of June 2010 is associated with a clear functional genomic footprint. Of the 3,296 genes included in our analysis, expression of 1,600 and 1,257 genes varied among field sites and throughout the time course, respectively ($P < 0.01$) (Dataset S3). For the 646 genes that varied in expression only among sites (no significant time effect or site-by-time interaction), site variation followed a pattern of population isolation by distance, which is consistent with neutral evolutionary divergence (Fig. 2*A*) and population genetic expectations (15). Most importantly, 1,500 genes indicated a pattern of site-dependent time course expression (significant interaction, false discovery rate <0.01), where the trajectory of genome expression through time was divergent at the GT site compared with all other sites (Fig. 2 *B* and *C)*, particularly at the second time point, which coincides with oil contamination (Fig. 1*C*).

Previous studies have identified genes that are transcriptionally responsive to planar polychlorinated biphenyl (PCB) exposures in killifish (16). Planar PCBs, dioxins, and PAHs (the primary toxic constituents in crude oil) are all mechanistically related insofar as they exert biological effects, in whole or in part, through aryl-hydrocarbon receptor (AHR) signaling pathways; indeed, morpholino knockdown of the AHR is protective of the toxic effects of PAHs and PCBs in killifish (17), and exposures to PCBs and PAHs induce common genome expression responses in flounder (18). Of the genes that were transcriptionally responsive to PCB exposures (16), 380 were included in the current analysis. Expression of this subset of genes is predictive of transcriptional divergence in fish from the GT site coincident with oil contamination compared with other field sites (Fig. S3), especially for the top 10% of PCB-responsive genes (Fig. 2*D*). Transcriptional activation of these planar PCB-responsive genes in developing killifish embryos is predictive of induction of developmental abnormalities, decreased hatching success, and decreased embryonic and larval survival (16, 19). This set of genes includes members of the canonical battery of genes that are transcriptionally induced by ligand-activated AHR signaling, such as cytochrome P450s, cytochrome B5, and UDP-glucuronosyltransferase (Fig. 2*F*, set 1), for which increased transcription is particularly diagnostic of exposure to select hydrocarbons (20). Indeed, many genes that are transcriptionally induced or repressed by AHR activators (dioxins, PCBs, and PAHs) show induction or repression at the GT site coincident with crude oil contamination (Fig. 2*F*, set 1). An independent measure of genome expression, RNAseq, also indicates AHR activation in GT fish from June 28, 2010, compared with reference RNA (e.g., up-regulation of cytochrome P450s, UDP-glucuronosyltransferase (UGT), and AHR itself; Fig. 2*E*). In parallel, up-regulation of CYP1A protein was detected in gills from GT fish sampled postoil and in early life-stage fish following controlled exposures to GT waters (Figs. 3 and 4). These data appear to be diagnostic of exposure to the toxic constituents in contaminating oil (PAHs) at a sufficient concentration and duration to induce biological responses in resident fish. Sustained activation of the CYP1A gene (Figs. 2*F* and 3) was predictive of persistent exposure to sublethal concentrations of crude oil components and negative population-level impacts in fish, sea otters, and harlequin ducks following the *Exxon Valdez* oil spill (reviewed in 1), although PAH toxicity may be mediated through AHR-independent pathways as well (21).

Transcriptional responses in other sets of coexpressed genes offer insights into the potential biological consequences of contaminating oil exposure at the GT site. Several gene ontology (GO) categories were enriched in the subset of genes that showed GT-specific expression divergence coincident with site- and time-specific oil contamination (Dataset S4). GO enrichment indicates activation of the ubiquitin-proteasome system (Fig. 2*F*, set 2), which, among diverse functions, is important for cellular responses to stress, cell cycle regulation, regulation of DNA repair, apoptosis, and immune responses (22). The AHR protein itself plays a role as a unique ligand-dependent E3 ubiquitin ligase that targets sex steroid (estrogen and androgen) receptor proteins for proteasomal destruction, thereby impairing

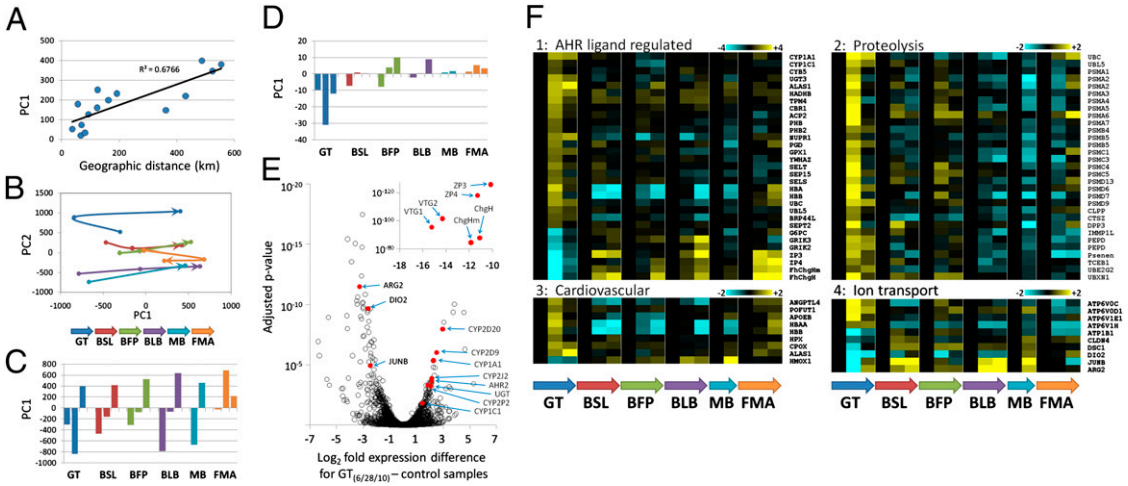

Fig. 2. Genome expression between field sites and across time. Field sites include Grand Terre (GT), Bay St. Louis (BSL), Belle Fontaine Point (BFP), Bayou La Batre (BLB), Mobile Bay (MB), and Fort Morgan (FMA). GT was the only site to be directly oiled, which occurred between the first and second sampling times (Fig. 1 and Dataset S2). (*A*) For genes that vary only among sites (no expression change with time or interaction), pairwise site-specific transcriptome divergence along principal component (PC) 1, as a function of pairwise geographical distance, shows a pattern consistent with isolation by distance. (*B*) Trajectory of genome expression responses through time for each of six field sites from the preoil sample time (dot at base of arrow) through the peak-oil sample time (middle dot), to the latest postevent sample time (dot at head of arrow) following PC analysis of genes showing statistically significant main effects (site and time) and interaction terms. (*C*) Divergence along PC1 is isolated, where bars for each site from left to right represent sampling times from the earliest to the latest. (*D*) Expression divergence along PC1 for the subset of genes that is dose-responsive to PCB exposure (top 10% of PCB-responsive genes). (*E*) RNAseq data showing genes up- and down-regulated (*x* axis positive and negative, respectively) in fish from GT sample time 2 (coincident with oil) compared with reference RNA, where select genes are identified. (*Inset*) Genes are dramatically down-regulated at GT (detailed RNAseq data are presented in Dataset S5). (*F*) Expression levels for specific genes (rows) and treatments (columns), where cell color indicates up-regulation (yellow) or down-regulation (blue) scaled according to site-specific expression level at the preoil sample time, for genes with divergent expression at the GT site. Genes are grouped into functional categories, and scale bars indicate *N*-fold up- or down-regulation.

normal cellular responses to sex hormones in reproductive tissues, and this response can be activated by planar PAHs (23). Significant down-regulation of transcripts for egg envelope proteins zona pellucida (ZP3 and ZP4) and choriogenin (ChgHm and ChgH) that we detect at the GT site coincident with oil exposure (Fig. 2*F*, set 1) may be linked to this AHR-dependent proteolytic pathway because their transcription is estrogen-dependent (24, 25) and is down-regulated by exposure to PAHs in fish (25–27). In corroboration, RNAseq detects dramatically down-regulated ZP, ChgH, and vitellogenin transcripts in GT fish (Fig. 2*E*). Although the transcriptional response that we detect is in male fish, these proteins are synthesized in male livers (reviewed in 25, 27) and down-regulation is consistent with antiestrogenic effects from exposure to PAHs (28). Possible impacts on reproduction merit attention because water only from the GT site induced CYP1A protein in the gills of developing killifish (Fig. 3) at low concentrations of total aromatics and alkanes (Dataset S2) and more than 2 mo after initial oiling, indicating persistent bioavailability of PAHs. Marsh contamination with DWH oil coincided with the spawning season for many marsh animals, including killifish (29), and reproductive effects are predictive of long-term population-level impacts from oil spills (1).

Controlled exposures of developing killifish to water collected from GT on June 28 and August 30, 2010, induced CYP1A protein expression in larval gills relative to fish exposed to GT water preoil and exposed to Bayou La Batre (BLB) site water that was not oiled (Fig. 3). This response is consistent with the location and timing of oil contamination, and it indicates that the remaining oil constituents dissolved at very low concentrations at GT after landfall (Dataset S2) were bioavailable and bioactive to developing fish. Although exposures to PAHs stereotypically induce cardiovascular system abnormalities in developing fish at relatively high concentrations (e.g., 21), none were observed in these animals. However, even very low-concentration exposures during development, insufficient to induce cardiovascular abnormalities in embryos, can impair cardiac performance in adulthood (30). The adult fish sampled in situ from the oil-contaminated GT site showed divergent regulation of several genes involved in blood vessel morphogenesis and heme metabolism coincident with oil contamination (Fig. 2*F*, set 3). Multigeneration field studies are necessary to confirm cardiovascular effects from DWH oil contamination of marshes that coincided with spawning.

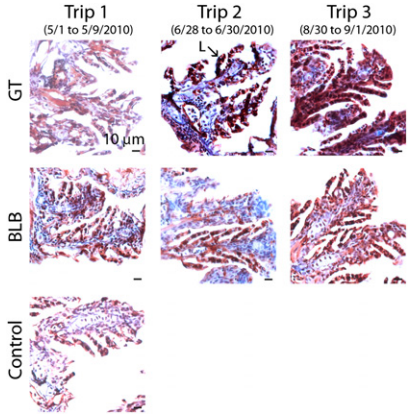

Fig. 3. CYP1A protein expression (dark red staining) in larval killifish gills (24 d postfertilization) exposed to waters collected from GT (oiled) and BLB (not oiled) during development. (Magnification 40×, scale bars = 10 μm.) CYP1A expression is elevated in the lamellae of larvae exposed during development to waters collected from GT postoil (trips 2 and 3) compared with background levels of CYP1A expression in larvae exposed to GT water preoil (trip 1), compared with CYP1A in fish exposed to waters collected from BLB (which was not directly oiled), and compared with CYP1A in fish reared in laboratory control water. Nuclei were stained using hematoxylin (blue). Analytical chemistry of exposure waters is reported in Dataset S2.

Coastal salt marsh habitats are dynamic and stressful, where changes in environmental parameters, such as temperature, hypoxia, and salinity, can continuously challenge resident wildlife. Regulation of ion transport in fish is particularly important for facilitating homeostasis in response to the salinity fluctuations that are common in estuaries. We found altered regulation of multiple ion transport genes in fish from the GT site coincident with oil contamination (Fig. 2*F*, set 4). For example, V-type proton ATPases are up-regulated and Na^+,K^+-ATPase subunits and tight-junction proteins are down-regulated, coincident with oiling at the GT site, in the absence of substantial changes in environmental salinity (Dataset S2). Other genes important for osmotic regulation in killifish (31) are also divergently down-regulated at the GT site, including type II iodothyronine deiodinase (DIO2), transcription factor jun-B (JUNB), and arginase 2 (ARG2). In corroboration, RNAseq data show down-regulation of DIO2, JUNB, and ARG2 in GT fish compared with reference fish (Fig. 2*E*). Although the physiological consequences of oil exposures are typically studied in isolation, it is reasonable to predict that exposure to oil may compromise the ability of resident organisms to adjust physiologically to natural stressors.

Induction of CYP1A protein expression is a hallmark of AHR signaling pathway activation, making it a sensitive biomarker of exposure to select planar PAHs and other hydrocarbons (20). Although the liver is the key organ for CYP1A-mediated metabolism of these substrates, gill tissues represent the most proximate site of exposure to PAHs. As a result of direct contact with the environment and the nature of the gill as a transport epithelium, the gill may be a more sensitive indicator of exposure to contaminants than the liver (32). CYP1A protein was markedly elevated in GT fish postoil compared with GT fish preoil and compared with fish from other field sites that were not directly oiled (Fig. 4). CYP1A induction was localized predominantly to pillar cells of the gill lamellae and within undifferentiated cells underlying the interlamellar region, which may have contributed to the filamental and lamellar hyperplasia observed during trips 2 and 3, as well as the gross proliferation of the interlamellar region observed during trip 2 in GT fish (Fig. 4). These effects imply a decrease in the effective surface area of the gill, a tissue that supports critical physiological functions, such as ion homeostasis, respiratory gas exchange, systemic acid-base regulation, and nitrogenous waste excretion (33). Currently, the degree to which oil-induced effects may interact with commonly encountered challenges, such as fluctuations in hypoxia and salinity, to compromise physiological resilience is unclear.

By integrating remote sensing and in situ chemical measures of exposure, and linking these with integrated measures of biological effect (genome expression and tissue morphology), we provide evidence that links biological impacts with exposure to contaminating oil from the DWH spill within coastal marsh habitats. Although body burdens of toxins are not high, consistent with reports indicating that seafood from the Gulf of Mexico is safe for consumption (34), this does not mean that negative biological impacts are absent. Our data reveal biologically relevant sublethal exposures causing alterations in genome expression and tissue morphology suggestive of physiological impairment persisting for over 2 mo after initial exposures. Sublethal effects were predictive of deleterious population-level impacts that persisted over long periods of time in aquatic species following the *Exxon Valdez* spill (1) and must be a focus of long-term research in the Gulf of Mexico, especially because high concentrations of hydrocarbons in sediments (Dataset S2) may provide a persistent source of exposures to organisms resident in Louisiana marshes.

Methods

The locations (latitude and longitude) of our field sampling sites and dates for sampling at each site are summarized in Dataset S1. Gulf killifish (*F. grandis*) were caught by minnow trap, and tissues were excised immediately. Liver was preserved in RNAlater (Ambion, Inc.) for genome expression (microarray and RNAseq) analysis. Gill tissues were fixed in situ in buffered zinc-based formalin Z-Fix (Anatech LTD). Succinct methods follow, and more detailed methods are available online.

Satellite imagery (SAR) was analyzed to provide estimation of the timing, location, and duration of coastal oil contamination. The calculated distance from each field sampling site to the nearest oil slick was calculated from the "straight-line" distance from the global positioning system position of the station (Dataset S1) to that of the observed oil across any and all intervening geographical barriers (e.g., Fig. S1).

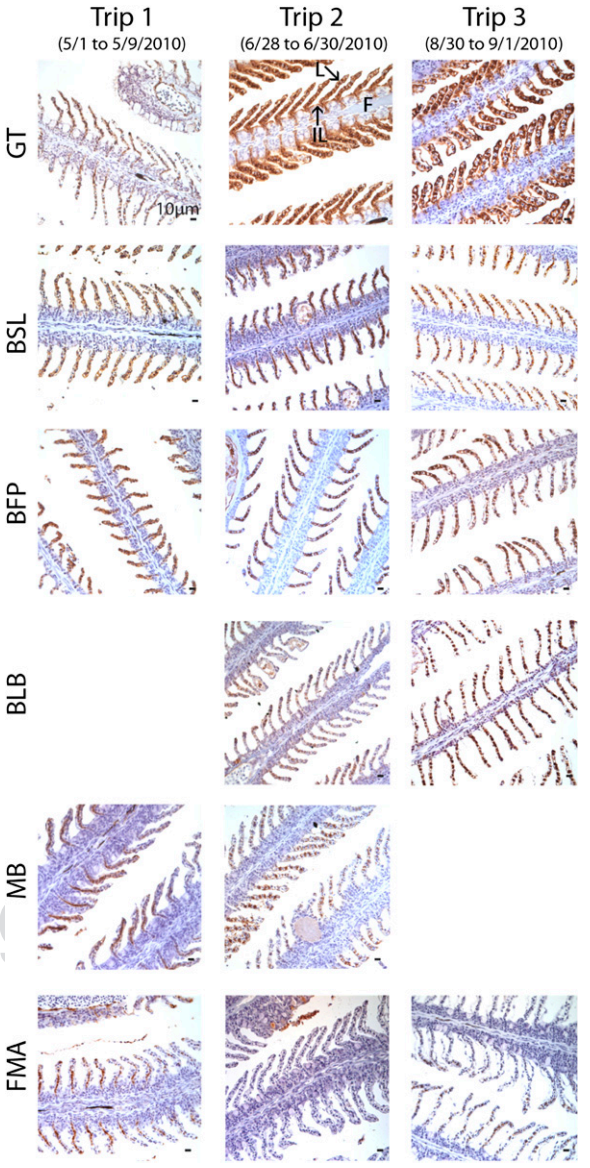

Fig. 4. CYP1A protein expression in adult killifish gills (dark red staining) sampled in situ from all sampling times (columns) and locations (rows). Locations include Grand Terre (GT), Bay St. Louis (BSL), Belle Fontaine Point (BFP), Bayou La Batre (BLB), Mobile Bay (MB), and Fort Morgan (FMA). (Magnification 40×, scale bars = 10 μm.) The MB site was only sampled on trips 1 and 2, and gills from trip 1 at the BLB site were not available for processing. Fish gills from the GT site during trips 2 and 3 showed high CYP1A expression and an elevated incidence of hyperplasia of the lamellae and interlamellar space on the gill filaments coincident with oil contamination. CYP1A protein was elevated at the GT site postoil (trips 2 and 3) compared with GT preoil (trip 1) as well as with other field sites, none of which were directly oiled. Nuclei were stained using hematoxylin (blue). Exact site locations and sampling dates are reported in Dataset S1.

Analytical chemistry of water, tissue, and sediment samples was performed to offer detailed characterization of exposure to contaminating oil (data reported in Dataset S2). Sample dates and locations are summarized in Dataset S1. All sample extracts were analyzed using GC interfaced to an MS detector system. Spectral data were processed by Chemstation Software (Agilent Technologies), and analyte concentrations were calculated based on the internal standard method.

Genome expression across sites and time was characterized using custom oligonucleotide microarrays. Genome expression was measured in liver tissues from five replicate individual male fish per site-time treatment (5 biological replicates) hybridized in a loop design, including a dye swap. Data were lowess-normalized and then mixed model-normalized using linear mixed models to account for fixed (dye) effects and random (array) effects. Normalized data were then analyzed using mixed model ANOVA, with "site" [Grand Terre (GT), Bay St. Louis (BSL), Belle Fontaine Point (BFP), Bayou La Batre (BLB), Mobile Bay (MB), and Fort Morgan (FMA)] and "sampling time" (sampling trips 1, 2, and 3) (Dataset S1) as main effects, including an interaction (site-by-time) term. The false discovery rate was estimated using Q-value (35). Principal components analysis was performed using MeV (36). GO enrichment was tested using DAVID (37).

For RNAseq, transcript abundance was compared between liver mRNA from three replicate fish (RNA was not pooled) from the GT site from June 28, 2010, and mRNA from two control samples. All RNA samples were sequenced on the Illumina Gene Analyzer platform (Expression Analysis, Inc.). Following quality control filtering, quantitative transcript abundance analysis was performed by mapping sequence reads to target sequences (6,810 unique *F. heteroclitus* target EST sequences, Dataset S5) using the Bowtie short read alignment software (38). A custom Perl script determined the number of fragments mapped to each target sequence. The Bioconductor package DESeq (version 2.8) (39) was used to determine the statistical significance of each differentially expressed target using a negative binomial method with *P* values adjusted by the Benjamini–Hochberg procedure.

Gill tissues were sampled from all field sites for morphological analysis and immunohistochemical analysis of CYP1A protein expression. Gill tissues from the first and second gill arches were sectioned along the longitudinal axis at a thickness of 4 μm and probed with mAb C10-7 against fish CYP1A (40). Sections were counterprobed using the Vectastain ABC immunoperoxidase system (Vector Laboratories), utilizing the ImmPACT Nova RED peroxidase substrate kit (Vector Laboratories) to visualize the CYP1A protein in red. Tissue sections were counterstained with Vector Hematoxylin QS (Vector Laboratories).

F. grandis embryos obtained from parents not exposed to oil (collected from Cocodrie, LA) were exposed to water samples from the GT and BLB sites collected subsurface on the dates indicated in Dataset S1. Following fertilization, 20 embryos were randomly transferred in triplicate to one of the six field-collected waters (2 field sites × 3 time points) at 3 h postfertilization. Embryos were also exposed to a laboratory control consisting of artificial 17 parts per thousand (ppt) water. Larvae were sampled at 24 d postfertilization and fixed in Z-Fix solution. Sectioning and staining were as described in the previous section.

ACKNOWLEDGMENTS. K. Carman helped facilitate early field studies. The authors thank R. Brennan, D. Roberts, E. McCulloch, Y. Meng, A. Rivera, C. Elkins, H. Graber, R. Turner, D. Crawford, and M. Oleksiak, for technical assistance. Funding was from the National Science Foundation (Grants DEB-1048206 and DEB-1120512 to A.W., Grant EF-0723771 to A.W. and F.G., and Grant DEB-1048241 to R.B.W.), the National Institutes of Health (R15-ES016905-01 to C.D.R.), and the Gulf of Mexico Research Initiative (A.W., F.G., and N.W.).

1. Peterson CH, et al. (2003) Long-term ecosystem response to the Exxon Valdez oil spill. *Science* 302:2082–2086.
2. Rozas LP, Reed DJ (1993) Nekton use of marsh-durface habitats in Louisiana (USA) deltaic salt marshes undergoing submergence. *Mar Ecol Prog Ser* 96:147–157.
3. Rozas LP, Zimmerman RJ (2000) Small-scale patterns of nekton use among marsh and adjacent shallow nonvegetated areas of the Galveston Bay Estuary, Texas (USA). *Mar Ecol Prog Ser* 193:217–239.
4. Subrahmanyam CB, Coultas CL (1980) Studies on the animal communities in 2 North Florida salt marshes. 3. Seasonal fluctuations of fish and macroinvertebrates. *Bull Mar Sci* 30:790–818.
5. Lotrich VA (1975) Summer home range and movements of *Fundulus heteroclitus* (Pisces: Cyprinodontidae) in a tidal creek. *Ecology* 56:191–198.
6. Teo SLH, Able KW (2003) Habitat use and movement of the mummichog (*Fundulus heteroclitus*) in a restored salt marsh. *Estuaries* 26:720–730.
7. Van Veld PA, Nacci DE (2008) Toxicity resistance. *The Toxicology of Fishes*, eds Di Giulio RT, Hinton DE (Taylor and Francis, Boca Raton, FL), pp 597–641.
8. Whitehead A (2010) The evolutionary radiation of diverse osmotolerant physiologies in killifish (*Fundulus* sp.). *Evolution* 64:2070–2085.
9. Able KW, Hata D (1984) Reproductive behavior in the *Fundulus heteroclitus-F. grandis* complex. *Copeia* (4):820–825.
10. Kneib RT (1997) The role of tidal marshes in the ecology of estuarine nekton. *Oceanography and Marine Biology: An Annual Review* 35:163–220.
11. Nordlie FG (2006) Physicochemical environments and tolerances of cyprinodontoid fishes found in estuaries and salt marshes of eastern North America. *Reviews in Fish Biology and Fisheries* 16:51–106.
12. Rozas LP, Lasalle MW (1990) A comparison of the diets of Gulf killifish, *Fundulus grandis* Baird and Girard, entering and leaving a Mississippi brackish marsh. *Estuaries* 13:332–336.
13. Weisberg SB, Lotrich VA (1982) The importance of an infrequently flooded intertidal marsh surface as an energy source for the mummichog *Fundulus heteroclitus*: An experimental approach. *Mar Biol* 66:307–310.
14. Brekke C, Solberg AHS (2005) Oil spill detection by satellite remote sensing. *Remote Sensing of Environment* 95:1–13.
15. Williams DA, Brown SD, Crawford DL (2008) Contemporary and historical influences on the genetic structure of the estuarine-dependent Gulf killifish *Fundulus grandis*. *Mar Ecol Prog Ser* 373:111–121.
16. Whitehead A, Pilcher W, Champlin D, Nacci D (2011) Common mechanism underlies repeated evolution of extreme pollution tolerance. *Proc R Soc B*, 10.1098/rspb.2011.0847.
17. Clark BW, Matson CW, Jung D, Di Giulio RT (2010) AHR2 mediates cardiac teratogenesis of polycyclic aromatic hydrocarbons and PCB-126 in Atlantic killifish (*Fundulus heteroclitus*). *Aquat Toxicol* 99:232–240.
18. Williams TD, et al. (2008) Transcriptomic responses of European flounder (Platichthys flesus) to model toxicants. *Aquat Toxicol* 90:83–91.
19. Whitehead A, Triant DA, Champlin D, Nacci D (2010) Comparative transcriptomics implicates mechanisms of evolved pollution tolerance in a killifish population. *Mol Ecol* 19:5186–5203.
20. Varanasi U (1989) *Metabolism of Polycyclic Aromatic Hydrocarbons in the Aquatic Environment* (CRC, Boca Raton, FL), p 341.
21. Incardona JP, et al. (2005) Aryl hydrocarbon receptor-independent toxicity of weathered crude oil during fish development. *Environ Health Perspect* 113:1755–1762.
22. Glickman MH, Ciechanover A (2002) The ubiquitin-proteasome proteolytic pathway: Destruction for the sake of construction. *Physiol Rev* 82:373–428.
23. Ohtake F, et al. (2007) Dioxin receptor is a ligand-dependent E3 ubiquitin ligase. *Nature* 446:562–566.
24. Modig C, et al. (2006) Molecular characterization and expression pattern of zona pellucida proteins in gilthead seabream (Sparus aurata). *Biol Reprod* 75:717–725.
25. Yu RMK, Wong MML, Kong RYC, Wu RSS, Cheng SH (2006) Induction of hepatic choriogenin mRNA expression in male marine medaka: A highly sensitive biomarker for environmental estrogens. *Aquat Toxicol* 77:348–358.
26. Holth TF, et al. (2008) Differential gene expression and biomarkers in zebrafish (*Danio rerio*) following exposure to produced water components. *Aquat Toxicol* 90:277–291.
27. Sanchez BC, Carter B, Hammers HR, Sepúlveda MS (2011) Transcriptional response of hepatic largemouth bass (Micropterus salmoides) mRNA upon exposure to environmental contaminants. *J Appl Toxicol* 31:108–116.
28. Thomas P (1990) Teleost model for studying the effects of chemicals on female reproductive endocrine function. *J Exp Zool Suppl* 4(Suppl 4):126–128.
29. Greeley MS, Macgregor R (1983) Annual and semilunar reproductive-cycles of the Gulf killifish, *Fundulus grandis*, on the Alabama Gulf Coast. *Copeia* (3):711–718.
30. Hicken CE, et al. (2011) Sublethal exposure to crude oil during embryonic development alters cardiac morphology and reduces aerobic capacity in adult fish. *Proc Natl Acad Sci USA* 108:7086–7090.
31. Whitehead A, Roach JL, Zhang S, Galvez F (2011) Genomic mechanisms of evolved physiological plasticity in killifish distributed along an environmental salinity gradient. *Proc Natl Acad Sci USA* 108:6193–6198.
32. Levine SL, Oris JT (1999) CYP1A expression in liver and gill of rainbow trout following waterborne exposure: Implications for biomarker determination. *Aquat Toxicol* 46:279–287.
33. Evans DH, Piermarini PM, Choe KP (2005) The multifunctional fish gill: Dominant site of gas exchange, osmoregulation, acid-base regulation, and excretion of nitrogenous waste. *Physiol Rev* 85:97–177.
34. State of Louisiana Department of Health and Hospitals (2011) *Louisiana Seafood Safety Surveillance Report* (Louisiana Department of Health and Hospitals, Baton Rouge, LA).
35. Storey JD, Tibshirani R (2003) Statistical significance for genomewide studies. *Proc Natl Acad Sci USA* 100:9440–9445.
36. Saeed AI, et al. (2006) TM4 microarray software suite. *Methods Enzymol* 411:134–193.
37. Huang W, Sherman BT, Lempicki RA (2009) Systematic and integrative analysis of large gene lists using DAVID bioinformatics resources. *Nat Protoc* 4:44–57.
38. Langmead B, Trapnell C, Pop M, Salzberg SL (2009) Ultrafast and memory-efficient alignment of short DNA sequences to the human genome. *Genome Biol* 10:R25.
39. Anders S, Huber W (2010) Differential expression analysis for sequence count data. *Genome Biol* 11:R106.
40. Rice CD, Schlenk D, Ainsworth J, Goksoyr A (1998) Cross-reactivity of monoclonal antibodies against peptide 277-294 of rainbow trout CYP1A1 with hepatic CYP1A among fish. *Mar Environ Res* 46:87–91.

Supporting Information

Whitehead et al. 10.1073/pnas.1109545108

SI Methods

The locations (latitude and longitude) of our field sampling sites and dates for sampling at each site are summarized in Dataset S1. Gulf killifish (*Fundulus grandis*) were caught by minnow trap, and tissues were excised immediately. Liver was preserved in RNAlater (Ambion, Inc.) for genome expression (microarray and RNAseq) analysis. Gill tissues were fixed in situ in buffered zinc-based formalin Z-Fix (Anatech LTD).

Satellite Imagery. Satellite imagery was analyzed to provide a coarse but spatially and temporally comprehensive estimation of the timing, location, and duration of coastal oil contamination. Surface oil from the DWH oil spill was detected through the analysis of SAR images, which offer the most effective means of detecting oil remotely. This active radar system operates over large spatial scales in all weather and at all times of day (1, 2). Oil dampens the ocean's smallest capillary waves (3–5 cm in length), yielding black regions in the image attributable to the total lack of microwave backscatter from the sea surface to the sensor, compared with higher backscatter from surrounding regions with waves (Fig. S1). False-positive results are possible from areas with low wind (<3 m/s) and from algal blooms; thus, the use of another satellite sensor or "sea truth" (e.g., wind measurements) is advisable for confirmation of the SAR signal. Only SAR images with distinct signatures, unrelated to these potential artifacts, were used in this study, although even thin oil sheens would potentially yield a dark return because SAR data yield no information about oil thickness. We used SAR measurements from multiple satellites (TerraSARX; ERS-2; CosmoSkymed-1, -2, and -3; Radarsat-1 and -2; Palsar; and Envisat-2). Data were received and processed in real time at the University of Miami Center for Southeastern Tropical Advanced Remote Sensing (CSTARS) laboratory and were further processed at the Louisiana State University Earth Scan Laboratory. The calculated distance from each field sampling site to the nearest oil slick was calculated from the "straight-line" distance from the global positioning system position of the station (Dataset S1) to that of the observed oil across any and all intervening geographical barriers (e.g., Fig. S1). Therefore, calculated distances do not necessarily represent the overall distance oil would have traveled to reach a sample station, although as the calculated distance approaches zero, these two distances (straight line vs. travel distance) become extensionally equivalent.

Analytical Chemistry. Analytical chemistry of water, tissue, and sediment samples was performed to offer detailed characterization of exposure to contaminating oil (data reported in Dataset S2). Sample dates and locations are summarized in Dataset S1. Two liters of water was collected subsurface in 1-L amber-glass jars from each sample site and date, and it was kept at 4 °C until extraction, which was performed within 1 wk of collection. Tissues (whole fish) were collected from each of the field sites from the second (June 2010) and third (August 2010) sampling time points and frozen at −20 °C until extraction. Sediment was collected from each of the field sites after the final sampling time point (September 2010) in 8-oz glass jars and frozen at −20 °C until extraction.

The sediment extraction procedure is as follows. Approximately 30 g of sediment/soil was accurately weighed (to the nearest 0.01 g) into a precleaned 500-mL beaker. The material was homogenized with anhydrous sodium sulfate sample until a "dry" sand-like matrix was created. One milliliter of surrogate standard was spiked into the sample, followed by the addition of 100 mL of pesticide-grade dichloromethane (DCM). The sample mixture was sonicated (60% intensity) for ∼10 min and allowed to settle for 15 min. The solvent was poured over a sodium sulfate funnel to remove any water and drained into 500-mL flat-bottomed flasks. The extraction process was repeated two more times, followed by rinsing the funnel with 25 mL of DCM. The flask was placed on a Buchi evaporative system and reduced to a final volume of 5–10 mL of DCM. The DCM concentrate was pipetted from the flask, placed into a 10-mL microextraction thimble, and reduced to a final volume of 1 mL using a nitrogen blow-down system. The 1-mL extract was transferred to a 2-mL autosampler vial and spiked with 10 μL of internal standard solution. Autosampler vials were stored at 4 °C until ready for analysis.

The water extraction procedure is as follows. Approximately 1,000 mL of water was accurately weighed (to the nearest 1.0 mL) into a precleaned 20,000-mL separatory funnel. One milliliter of surrogate standard was spiked into the sample, followed by the addition of 100 mL of pesticide-grade DCM. The sample mixture was hand-shaken for ∼10 min and allowed to settle for 15 min. The solvent in the bottom of the funnel was drained through a sodium sulfate funnel to remove any water and drained into a 500-mL flat-bottomed flask. The extraction process was repeated two more times, followed by rinsing the funnel with 25 mL of DCM. The flask was placed on a Buchi evaporative system and reduced to a final volume of 5–10 mL of DCM. The DCM concentrate was pipetted from the flask, placed into a 10-mL microextraction thimble, and reduced to a final volume of 1 mL using a nitrogen blow-down system. The 1-mL extract was transferred to a 2-mL autosampler vial and spiked with 10 μL of internal standard solution. Autosampler vials were stored at 4 °C until ready for analysis.

The tissue extraction procedure is as follows. Approximately 5–10 g of tissue was accurately weighed to the nearest 0.01 g into a precleaned 500-mL beaker. The material was homogenized with anhydrous sodium sulfate sample until a dry sand-like matrix was created. One milliliter of surrogate standard was spiked into the sample, followed by the addition of 50 mL of pesticide-grade DCM. The sample mixture was sonicated (60% intensity) for ∼10 min and allowed to settle for 15 min. The solvent was poured over a sodium sulfate funnel to remove any water and drained into a 250-mL flat-bottomed flask. The extraction process was repeated two more times, followed by rinsing the funnel with 25 mL of DCM. The flask was placed on a Buchi evaporative system and reduced to a final volume of 3–5 mL of DCM. The DCM extract was exchanged to hexane with ∼25 mL of pesticide-grade hexane. The flask was returned to the evaporation system and evaporated down to a final volume of 2–5 mL of hexane. The sample was fractionated on an alumina/silica gel column by placing the 2- to 5-mL hexane aliquot on the aluminum/silica gel column, which was then rinsed with high-purity hexane. The flow of hexane was stopped before exposing the silica gel to air. This fraction, which contained alkanes, was collected in a graduated thimble. The alumina/silica gel column was then rinsed with 50% DCM and 50% hexane. The solvents were allowed to elute completely in a separate extraction thimble. This fraction contained the PAHs. The alkane and PAH fractions were combined and concentrated to 1.0 mL under a gentle stream of nitrogen and stored in a 2-mL autosampler vial (4 °C) until GC/MS analysis.

All sample extracts were analyzed using an Agilent 7890A Gas Chromatography system (Agilent Technologies, Inc.) config-

ured with a 5% diphenyl/95% (vol/vol) dimethyl polysiloxane high-resolution capillary column (30 m, 0.25-mm inner diameter, 0.25-μm film) directly interfaced to an Agilent 5975 inert XL MS detector system (Agilent Technologies, Inc.). An Agilent 7638B series Auto Injector (Agilent Technologies, Inc.) was used for sample introduction into the GC/MS system. The GC flow rates were optimized to provide a required degree of separation, which includes near-baseline resolution of n-C17 and pristine, and baseline resolution of n-C18 and phytane. The injection temperature was set at 250 °C, and only high-temperature and low-thermal bleed septa were used in the GC inlet. GC was performed in the temperature program mode with an initial column temperature of 55 °C for 3 min, which was then increased to 280 °C at a rate of 5 °C/min and held for 3 min. The oven was then heated from 280 °C to 300 °C at a rate of 1.5 °C/min and held at 300 °C for 2 min. Total run time was 66.33 min per sample. The interface to the MS was maintained at 280 °C. Ultra-high-purity helium was the carry gas for the GC/MS system.

Spectral data were processed by Chemstation Software (Agilent Technologies, Inc.). Analyte concentrations were calculated based on the internal standard method. Therefore, an internal standard mixture composed of naphthalene-d8, acenaphthene-d10, chrysene-dl2, and perylene-dl2 (usually at a concentration of 10 ng/μL) was spiked into the sample extracts just before analysis. The concentration of specific target oil analytes was determined by a five-point calibration and internal standard method. Standards containing parent (nonalkylated) hydrocarbons were used in the calibration curve. Alkylated homologs were quantified using the response factor of the parent, and were therefore semiquantitative. This was the standard procedure, because alkylated standards were not available.

Genome Expression: Microarrays. Genome expression across sites and time was characterized using custom oligonucleotide microarrays. Genome expression was measured in liver tissues from five replicate individual male fish per site-time treatment (5 biological replicates). Male fish were chosen for genome expression analysis because sampling was conducted during spawning season, when female reproductive condition (and associated liver genome expression) can be highly variable. Microarray probes (60-mer) were designed from contigs constructed from *F. heteroclitus*-expressed sequence tags. *F. heteroclitus* is the Atlantic coast-distributed sister species of Gulf coast-distributed *F. grandis* (3). Microarrays included probes for 6,800 unique EST sequences, each printed in duplicate on 15,000 element custom Agilent microarrays (design ID no. 027999) (Agilent Technologies, Inc.). Total RNA was extracted using TRIzol reagent, antisense RNA (aRNA) prepared using the amino allyl aRNA amplification kit (Ambion, Inc.), and purified aRNA coupled to Alexa Fluor dyes (Alexa Fluor 555 and 647; Molecular Probes, Inc.), and it was hybridized to custom microarrays for 18 h at 60 °C in a balanced loop design. Microarray images were captured using a Packard Bioscience ScanArray Express (PerkinElmer, Inc.) microarray scanner, and images were processed using Imagene (Biodiscovery, Inc.). Spots that were too bright (saturated) or too faint (below 2 SDs above background intensity) were excluded from normalization, resulting in a final set of 3,296 probes included for normalization and statistical analysis (Dataset S3). Data were lowess-normalized and then mixed model-normalized using linear mixed models to account for fixed (dye) effects and random (array) effects. Normalized data were then analyzed using mixed model ANOVA, with "site" [Grand Terre (GT), Bay St. Louis (BSL), Belle Fontaine Point (BFP), Bayou La Batre (BLB), Mobile Bay (MB), and Fort Morgan (FMA)] and "sampling time" (sampling trips 1, 2, and 3) (Dataset S1) as main effects, including an interaction (site-by-time) term. "Dye" was considered a fixed effect, and "array" and "replicate individual within site-time treatment" ($n = 5$) were treated as random effects. The false discovery rate was estimated using Q-value (4). Principal components analysis was performed using MeV (5). GO enrichment was tested using DAVID (6).

Genome Expression: RNAseq. Transcript abundance was compared between liver mRNA from three replicate fish (RNA was not pooled) from the GT site from June 28, 2010, and mRNA from two control samples. The two control samples are composed of pooled liver mRNA from six and eight individuals, respectively, collected in April 2008. The individuals for one control sample were collected (2 each) from three sites west of the Mississippi river, including Port Aransas, Texas; Cocodrie, Louisiana; and LeeVille, Louisiana. The individuals for the second control sample were collected (2 each) from four sites west of the Mississippi River, including Dauphin Island, Alabama; Weeks Bay, Alabama; Santa Rosa Island, Florida; and St. Teresa, Florida. All RNA samples were sequenced on the Illumina Gene Analyzer platform (Expression Analysis, Inc.), and the resulting short-read data were summarized in fastq format. Short reads with more than two uncalled bases were removed. Each read was cut whenever a position fell below a minimum quality score of 10 or if the average of the qualities of a position and its two neighbors fell below 20, and the largest remaining fragment was used.

Quantitative transcript abundance analysis was initiated by mapping filtered short reads to target sequences (6,810 unique *F. heteroclitus* target EST sequences, Dataset S5) using the Bowtie short read alignment software (7). A custom Perl script determined the number of fragments mapped to each target sequence. The Bioconductor package DESeq (version 2.8) (8) was then used to determine statistical significance of each differentially expressed target using a negative binomial method with *P* values adjusted by the Benjamini–Hochberg procedure. The three GT site samples were identified as a single "Exposed" class to DESeq, and the two pooled samples were identified as a single "Control" class.

Gill Morphology and Protein Expression: Field Study. Male and female fish were sampled from all field sites for analysis of CYP1A protein expression in the gills. Tissues were fixed immediately in Z-Fix, stored on ice, and held at room temperature before further processing. Gill tissues from at least three fish per site per sampling time were dehydrated in ascending grades of histology-grade ethanol. Tissues were then transferred to a t-butanol bath before clearing in Histochoice Clearing Agent (Amersco) and embedding in Paraplast (Sigma). Tissues were cut along the longitudinal axis at a thickness of 4 μm using an American Optical 820 microtome and transferred onto poly-L-lysine–coated microscope slides. After rehydration, tissues were processed for antigen retrieval by microwave in Tris-buffered saline (pH 9.0) and blocked. Tissues were then probed with mAb C10-7 against fish CYP1A (9). Sections were counterprobed using the Vectastain ABC immunoperoxidase system (Vector Laboratories), utilizing the ImmPACT Nova RED peroxidase substrate kit (Vector Laboratories) to visualize the CYP1A protein in red. Tissue sections were counterstained with Vector Hematoxylin QS (Vector Laboratories). Slides were then observed with a Leica DM RXA2 microscope (Leica Microsystems), and images were captured with a Spot Insight 4 megapixel camera (Diagnostic Instruments). Representative images were captured at a magnification of 40×.

Early Life-Stage Experiments. Approximately 20 L of water was collected (in coordination with collection of water for analytical chemistry; Dataset S2) subsurface from field sites on the dates indicated in Dataset S1. Water was stored in airtight stainless-steel soda kegs and kept at 4 °C until experiments were conducted. Water samples from GT and BLB were utilized in laboratory exposures of *F. grandis* embryos obtained by in vitro

fertilization using ova and spermatozoa collected from a brood stock of unexposed adult *F. grandis* derived from Cocodrie, Lousiana before oiling. Cocodrie parental stock fish were maintained at Louisiana State University, where they were held in the aquatics facility at the Department of Biological Sciences in 400-L tanks maintained at 17 parts per thousand (ppt) water (Instant Ocean) under recirculating conditions.

Following fertilization, 20 embryos were randomly transferred in triplicate to one of the six field-collected waters (2 field sites × 3 time points) at 3 h postfertilization. Embryos were also exposed to a laboratory control consisting of artificial 17 ppt water. Larvae at 24 d postfertilization were sampled and fixed in Z-Fix solution. After fixation, tissues were prepared, sectioned, and stained with the mAb C10-7, as described in the previous section.

1. Brekke C, Solberg AHS (2005) Oil spill detection by satellite remote sensing. *Remote Sensing of Environment* 95:1–13.
2. Fingas MF, Brown CE (1997) Review of oil spill remote sensing. *Spill Science and Technology Bulletin* 4:199–208.
3. Whitehead A (2010) The evolutionary radiation of diverse osmotolerant physiologies in killifish (*Fundulus* sp.). *Evolution* 64:2070–2085.
4. Storey JD, Tibshirani R (2003) Statistical significance for genomewide studies. *Proc Natl Acad Sci USA* 100:9440–9445.
5. Saeed AI, et al. (2006) TM4 microarray software suite. *Methods Enzymol* 411:134–193.
6. Huang W, Sherman BT, Lempicki RA (2009) Systematic and integrative analysis of large gene lists using DAVID bioinformatics resources. *Nat Protoc* 4:44–57.
7. Langmead B, Trapnell C, Pop M, Salzberg SL (2009) Ultrafast and memory-efficient alignment of short DNA sequences to the human genome. *Genome Biol* 10:R25.
8. Anders S, Huber W (2010) Differential expression analysis for sequence count data. *Genome Biol* 11:R106.
9. Rice CD, Schlenk D, Ainsworth J, Goksoyr A (1998) Cross-reactivity of monoclonal antibodies against peptide 277-294 of rainbow trout CYP1A1 with hepatic CYP1A among fish. *Mar Environ Res* 46:87–91.

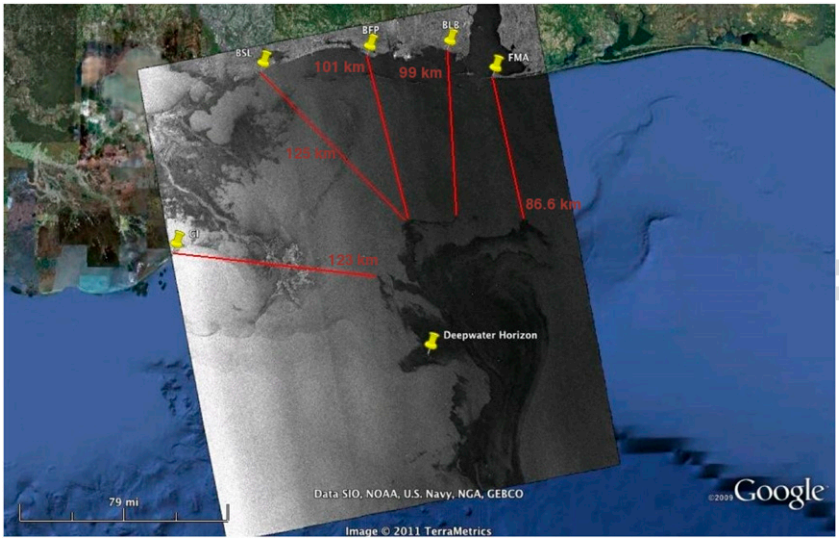

Fig. S1. Representative measurements of the distance from field sites to ocean surface oil according to the CosmoSkymed2 SAR image captured May 13, 2010, at 11:56 UTC (Coordinated Universal Time). Field sites include Grand Terre (GT), Bay St. Louis (BSL), Belle Fontaine Point (BFP), Bayou La Batre (BLB), and Fort Morgan (FMA).

Fig. S2. Oil contaminating the marsh at the GT field site on June 16, 2010 (photograph by B.D.).

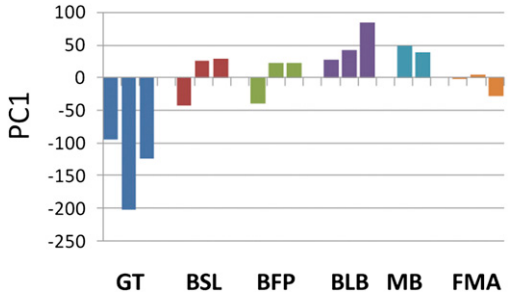

Fig. S3. Expression divergence along principal component 1 (PC1) across consecutive sampling times for the subset of 380 genes that was dose-responsive to PCB exposure in a study by Whitehead et al. (1). Field sites include Grand Terre (GT), Bay St. Louis (BSL), Belle Fontaine Point (BFP), Bayou La Batre (BLB), and Fort Morgan (FMA).

1. Whitehead A, Pilcher W, Champlin D, Nacci D (2011) Common mechanism underlies repeated evolution of extreme pollution tolerance. *Proc R Soc B*, 10.1098/rspb.2011.0847.

Dataset S1. Sites, precise locations, and sampling dates for three field sampling trips

Dataset S1

Dataset S2. Analytical chemistry of subsurface water samples, tissue samples (whole fish), and sediment samples

Dataset S2

Dataset S3. Genome expression microarray data: All probes included in the analysis, including the target EST sequence, probe sequence, annotation, average expression within each treatment (average of $n = 5$ replicate samples within each site-by-time treatment), and results from statistical analyses

Dataset S3

Dataset S4. Results of GO enrichment analysis using DAVID for the subset of genes that were divergently expressed at the GT site coincident with oil contamination

Dataset S4

Dataset S5. Genome expression RNAseq data: All gene targets included in the analysis, including the target EST sequence, annotation, fold difference in transcript abundance between the average of three replicate fish from GT sample time 2 (June 28, 2010) and two replicate reference RNA pools, and adjusted *P* values

Dataset S5